DMD Fast Forward. Published on September 11, 2008 as doi:10.1124/dmd.108.022764

Lacteal Secretion, Fetal and Maternal Tissue Distribution of Dasatinib in Rats

Kan He, Michael W. Lago, Ramaswamy A. Iyer, Wen-Chyi Shyu, William G. Humphreys, and Lisa J. Christopher

Departments of Pharmaceutical Candidate Optimization (K.H., R.A.I., W.C.S., W.G.H., L.J.C.), and Radiochemistry (M.W.L), Bristol-Myers Squibb Co., Princeton, NJ 08543

DMD Fast Forward. Published on September 11, 2008 as DOI: 10.1124/dmd.108.022764
This article has not been copyedited and formatted. The final version may differ from this version.

Running title: Lacteal Secretion and Fetal Tissue Distribution of Dasatinib

Corresponding author and current address:

Kan He

UniTris Biopharma Co.

399 Cailun Rd, Building 1, Zhangjiang Hi-Tech Park

Shanghai 201203, China

Phone: (86) 21-51320617, E-mail: kan.he@unitrispharma.com

Number of text pages: 29

Number of table: 2

Number of figure: 5

Number of reference: 26

Number of words in abstract: 250

Number of words in introduction: 426

Number of words in discussion: 935

ABBREVIATIONS: AUC, area under concentration–time curve; $AUC_{0\text{-}inf}$, area under concentration–time curve from 0 to infinity; $AUC_{(0\text{-}t)}$, area under concentration–time curve from 0 to the last measurable time point; BCRP, breast cancer resistance protein; C_{max}, maximum concentration; LC-MS/MS, liquid chromatography-tandem mass spectrometry; LSC, Liquid scintillation counting; QWBA, quantitative whole-body autoradiography; T_{max}, time at which maximum concentration occurs.

DMD Fast Forward. Published on September 11, 2008 as DOI: 10.1124/dmd.108.022764
This article has not been copyedited and formatted. The final version may differ from this version.

ABSTRACT

Dasatinib (SPRYCEL®, BMS-354825) is a potent and broad spectrum kinase inhibitor, used for the treatment of chronic myeloid leukemia and Philadelphia chromosome positive (Ph+) acute lymphoblastic leukemia. Dasatinib exhibited extensive lacteal secretion in Sprague-Dawley rats following a single oral dose of [^{14}C]dasatinib (10 mg/kg, 300 μCi/kg). Radioactivity was detected through 72 hours post-dose, with a milk/plasma $AUC_{0\text{-}inf}$ ratio of approximately 25. The majority of the total radioactivity in milk was attributed to unchanged dasatinib. Following a single dose of [^{14}C]dasatinib to pregnant Sprague-Dawley rats at gestation day 18, radioactivity was extensively distributed in maternal tissues. The radioactivity detected by tissue excision or quantitative whole body autoradiography was highest in adrenal gland, mammary tissue, lungs, kidneys, liver and placenta. Compared with maternal tissues, a relatively low level of radioactivity was detected in fetal tissues. The concentrations of dasatinib-equivalents in fetal liver and kidneys were <13% of the respective maternal organs. The C_{max} of dasatinib-equivalents in fetal blood was approximately 39% of that in maternal blood, however, the AUC values were comparable. Fetal brain/blood ratios of C_{max} and $AUC_{0\text{-}inf}$ were approximately 1.58 and 1.48, respectively, which were much greater than the maternal ratios of 0.12 and 0.13. In summary, dasatinib was extensively distributed in maternal tissues and secreted into milk, but its penetration into the adult brain was limited. Transporters may be involved in mediating dasatinib distribution in the adult rat,

while in the fetus, tissue and blood exposures were similar, suggesting that distribution in the fetus is predominantly mediated by diffusion.

Introduction

Dasatinib (SPRYCEL®, BMS-354825, Figure 1) is a potent, broad spectrum ATP-competitive inhibitor of 5 critical oncogenic tyrosine kinase families, including BCR-ABL, SRC, c-KIT, platelet-derived growth factor β receptor, and ephrin (EPH) receptor kinases (Lombardo et al., 2004; Schittenhelm et al., 2006; Tokarski et al., 2006). These kinases are involved in multiple forms of human malignancies (Daley et al., 1990; Lugo et al., 1990). Dasatinib is approximately 500-fold more potent than imatinib in inhibiting BCR-ABL. It binds to both the active and the inactive conformations of BCR-ABL, whereas imatinib only binds to the inactive state (Shah et al., 2006; Talpaz et al., 2006; Tokarski et al., 2006; Quintas-Cardama et al., 2007). In clinical trials, dasatinib induced rapid and long lasting major hematologic and cytogenetic responses in patients with imatinib-resistant or intolerant blast crisis chronic myeloid leukaemia (Guilhot et al., 2007; Hochhaus et al., 2007). Dasatinib also induced molecular responses, reducing BCR-ABL/ABL transcript ratios. Dasatinib is currently marketed for the treatment of adults with chronic, accelerated or blast phase chronic myeloid leukaemia with resistance or intolerance to prior therapy including imatinib mesylate, and for the treatment of adults with Philadelphia chromosome positive (Ph+) acute lymphoblastic leukaemia and lymphoid blast chronic myeloid leukaemia with resistance or intolerance to prior therapy. Dasatinib is also under clinical development for the treatment of solid tumors.

Dasatinib showed high intrinsic permeability in the Caco-2 cell model, however, the efflux ratio in this system was about 2-fold, suggesting that the compound may be a substrate for an intestinal efflux transporter (Kamath et al., 2008). Dasatinib showed a high volume of distribution (>3 L/kg) in each of the animal species (Kamath et al., 2008),

and was highly metabolized in rats, monkeys and humans (Christopher et al., 2008a; Christopher et al., 2008b). After IV administration of [^{14}C]dasatinib to bile duct-cannulated monkeys, approximately 10% and 67% of the dose was recovered in urine and bile, respectively. An additional 14% of the dose was recovered in feces, suggesting direct intestinal secretion of drug-derived radioactivity (Christopher et al., 2008a). Determining fetal and infant exposure to a drug as a consequence of maternal treatment is an important factor in evaluation of the risks associated with taking medication during pregnancy or while breast-feeding (Atkinson et al., 1988; Dorman et al., 2001). Studies with nursing and pregnant female rats are often utilized to obtain information on the potential for milk and placental transfer and fetal exposure (Solon and Kraus, 2002). The objectives of the current study were to investigate the lacteal secretion and maternal/fetal distribution of [^{14}C]dasatinib in rats after oral administration.

Material and Methods

Radiosynthesis of [^{14}C]-Dasatinib. [^{14}C]Dasatinib ([^{14}C]BMS-354825-08, lot No. 004) was synthesized at Bristol-Myers Squibb Co. (Princeton, NJ) (Allentoff et al., 2008). The specific activity was 31.9 μCi/mg and the radioactive purity was 98.7%.

Animal Welfare. Prior to study initiation, the protocol was approved by the Institutional Animal Care and Use Committee at Covance Laboratories Inc. (Madison, WI).

Test Animals, Housing and Randomization. Female Sprague Dawley rats (Harlan, Indianapolis, IN) on approximately 8-9 days postpartum were used for the lacteal secretion study. The rats weighed 287-351 g. Female Sprague Dawley rats on gestation day 18 were used for the maternal and fetal tissue distribution study. The rats weighed 258 to 355. For all studies, the animals were acclimated for at least 3 days prior to dose administration. During acclimation and the testing period, the animals were housed in individual polycarbonate shoe box cages. Certified Rodent Diet #8728CM (Harlan Teklad, Inc., Madison WI) and water were provided *ad libitum*.

Dose and Formulation. The dose was 10 mg/kg (300 μCi/kg) for the lacteal secretion study and the maternal and fetal tissue distribution studies. The oral dose was administered via a ball-tipped gavage needle. All control and pre-dose animals received dose vehicle only.

On the day before dose administration, a dosing solution was prepared by dissolving [^{14}C]dasatinib (2 mg/mL) in 6 mM hydrochloric acid in water (dose vehicle). The

formulation was stirred for 45 minutes and sonicated for 35 minutes. The pH of the resulting solution was 3.33. The dose formulation was stored at approximately 5°C and protected from light. On the day of dose administration, the dose formulation was removed from storage and sonicated for 30 minutes at approximately 66°C. Weighed aliquots in triplicate were taken from the top, middle, and bottom of each dose formulation before and after dose administration, and were analyzed by liquid scintillation counting (LSC) to determine the concentration of radioactivity and to verify homogeneity.

Lacteal Secretion. Milk was collected from 3 rats/time point at 1, 4, 8, 12, 24, 48, and 72 hours post-dose. Pups were removed from the mothers approximately 4 hours before collection of milk. Animals received a subcutaneous injection of oxytocin before milking to stimulate lactation. Animals were then anesthetized with ketamine, xylazine, and acepromazine cocktail immediately before the start of milk collection, and milk was collected using a specially constructed milking machine. Samples were immediately placed on ice or stored at approximately 5°C. The weight of each milk sample was recorded.

Following milk collection, animals were sacrificed by exsanguination (cardiac puncture) under isoflurane anesthesia and blood (as much as possible) was collected into tubes containing K_2EDTA. Blood was immediately placed on ice or stored at approximately 5°C and then centrifuged to obtain plasma.

DMD Fast Forward. Published on September 11, 2008 as DOI: 10.1124/dmd.108.022764
This article has not been copyedited and formatted. The final version may differ from this version.

Collection of organs and tissues by excision. For the maternal and fetal tissue distribution study, pregnant animals (3 animals/time point) were sacrificed by exsanguination (cardiac puncture) under isoflurane anesthesia at 1, 4, 8, 12, 24, 48, and 72 hours post-dose. Maternal blood (as much as possible) was collected into tubes containing K_2EDTA, and plasma was prepared by centrifugation at 1300 x g for 10 min. The following maternal tissues and organs were collected: cerebrum, heart, liver, kidneys, lungs, placenta, uterus, ovaries and amniotic fluid. The following fetal tissues were collected from two fetuses per dam: blood, brain, kidneys, liver, and residual fetus. Fetal blood was collected into heparinized tubes. All tissues except blood and milk were excised, rinsed with saline and blotted dry as appropriate, weighed, and then stored at -20°C until analysis. Blood samples were stored at approximately 5°C for radioanalysis and for plasma preparation. Milk samples were stored at approximately 5°C until radioanalysis, and then at approximately -20°C for LC-MS/MS analysis.

Sample Preparation and Measurement of Radioactivity. Plasma, milk and amniotic fluid samples were directly analyzed by LSC. Maternal and fetal blood samples were combusted and then analyzed by LSC. Ovaries, placenta, uterus, fetal brain, fetal kidney, fetal liver and residual fetus samples were digested and dissolved in sodium hydroxide and analyzed by LSC. Maternal kidney and liver samples were homogenized with a probe-type homogenizer, and the weighted aliquots were combusted and analyzed by LSC. Maternal cerebrum, heart and long samples were homogenized with a probe-type homogenizer, and the weighted aliquots were digested and dissolved in sodium hydroxide and analyzed by LSC.

All sample combustions were carried out in a Model 307 Sample Oxidizer (Packard Instrument Company, Meridan, CT) and the resulting $^{14}CO_2$ was trapped in a mixture of Perma Fluor and Carbo-Sorb. Radioactivity for all samples was determined by LSC with Ultima Gold XR scintillation cocktail in a model 2900TR liquid scintillation counter (Packard Instrument Company, Meridan, CT) for at least 5 minutes or 100,000 counts. All samples were analyzed in duplicate when sample size allowed. If results from sample duplicates (calculated as ^{14}C dpm/g sample) differed by more than 10% from the mean value, the sample was re-homogenized and re-analyzed (if the sample size permitted). This specification was met for all sample aliquots that had radioactivity greater than 100 dpm. Scintillation counting data (cpm) were automatically corrected for counting efficiency using the external standardization technique and an instrument-stored quench curve generated from a series of sealed quenched standards.

Metabolite profiling of milk samples by radiochromatographic analysis and LC-MS/MS. Pooled milk samples collected at 1, 4, 8, 12 or 24 h post-dose were used for metabolite profiling. The radioactivity in samples at 48 and 72 hours post-dose was not sufficient to produce meaningful profiles. Equal volumes of milk from each of the 3 animals at a given collection time were combined. The pooled milk samples were extracted 3 times with methanol/acetonitrile 1:1 (v/v), with a cumulative extraction recovery of >96% for all samples. Sample analyses were conducted on an Agilent 1100 HPLC system with a Phenomonex Synergi Polar-RP® column (4.6 x 250 mm, 4 μ, 80A) as described elsewhere (Christopher et al., 2008a; Christopher et al., 2008b). The mobile phase was 0.1% formic acid in water (A) and 0.1% formic acid in acetonitrile (B) in a stepped-gradient with a flow rate of 1 mL/min. For LC-radiochromatographic analysis, the column eluate was collected in Deepwell LumaPlate™-96-well plates (Perkin Elmer Biosciences, Downers Grove, IL) at 0.25 min intervals (0.25 mL/well) for 75 minutes after injection. The plates were dried overnight in a Speed Vac® (Savant Instruments Inc., Holbrook, NY) and counted for 10 min per well with a Packard Top Count NXT microplate scintillation analyzer (Perkin Elmer Biosciences, Downers Grove, IL). Radiochromatographic profiles for each of the pooled milk samples were constructed by plotting the radioactivity in each fraction against the time after injection. For LC/MS/MS identification of radioactive peaks, the column eluate was split with approximately 0.2 mL/min of the flow directed to a Finnigan LCQ Deca mass spectrometer (Thermo Fisher Scientific, Waltham, MA). Metabolites introduced into the mass-spectrometer by positive ion electrospray were identified on the basis of their mass spectral fragmentation

patterns and retention times in comparison to previously identified metabolites (Christopher et al., 2008a; Christopher et al., 2008b). The structures of the metabolites identified in milk samples are shown in Figure 1.

Quantitative Whole-Body Autoradiography (QWBA). Pregnant rats (one rat/time point) was sacrificed via an overdose of isoflurane anesthesia predose and at 1, 4, 8, 12, 24, 48, and 72 hours post-dose. Blood was collected into tubes containing K_2EDTA via right jugular venipuncture, and plasma was prepared by centrifugation at 1300 x g for 10 min. Aliquots of blood samples were maintained on wet ice or stored at approximately 5°C until analyzed. Immediately after blood collection, the animals were prepared for WBA.

The rat carcasses were immediately frozen in a hexane/dry ice bath for approximately 5 minutes. Each carcass was drained, blotted dry and stored at -70°C for at least 2 hours. Each carcass was then stored at -20°C. The frozen carcasses were individually embedded along with section thickness quality control standards (^{14}C-spiked rat blood) in chilled carboxymethylcellulose and frozen into blocks. Embedded carcasses were stored at -20°C in preparation for autoradiographic analysis. Appropriate sections were collected on adhesive tape at 40 µm thickness in a Leica CM 3600 cryomicrotome (Meyer Instruments, Houston, TX). Sections were collected at five levels of interest in the sagittal plane. All major tissues, organs, and biological fluids were represented. Collected sections were dried in the cryomicrotome chamber as appropriate. A section set from each animal was prepared by mounting a representative section from each level of interest. Mounted sections were tightly wrapped with mylar film and exposed on

Amersham Biosciences phosphorimaging screens along with plastic embedded ARC autoradiographic standards (American Radiolabeled Chemicals, St. Louis, MO). Screens were exposed for 4 days. Exposed screens were scanned using an Amersham Biosciences Storm™ PhosphorImager (Buckinghamshire, England). The autoradiographic images were analyzed using AIS software Version 4.0 (Imaging Research Inc, St. Catharine's Ontario, Canada). Specified tissues, organs, and fluids were analyzed. Tissue concentrations were interpolated from each standard curve as nanocuries/g and then converted to ng equivalents/g on the basis of the test article specific activity.

Data analysis. Pharmacokinetic parameters for distribution of radioactivity in organs and tissues were calculated from the excision data (n = 3 rats/time point). The parameters calculated included $t_{1/2}$, area under the concentration-time curve from time 0 to the last measurable time point (AUC_{0-t}), and area under the concentration-time curve from 0 to infinity (AUC_{0-inf}). The maximum concentration (C_{max}) was the highest concentration observed. Pharmacokinetic parameters were calculated by using WinNonlin Professional Edition, Version 4.1 (Pharsight Corporation, Mountain View, CA). The acceptance criteria for calculation of $t_{1/2}$ specified that the R-squared value must be >0.7.

Results

Lacteal Secretion. [^{14}C]-Dasatinib-derived radioactivity was extensively secreted in milk, with radioactivity detected at all time points through 72 hours post-dose. As shown in Figure 2, the concentration of dasatinib-equivalents in milk at each time point was

higher than that in plasma or blood. The milk/plasma concentration ratios ranged from 2.4 to 37.2. The milk $AUC_{0\text{-inf}}$ was approximately 25-fold greater than the plasma $AUC_{0\text{-inf}}$ (Table 1). The elimination $t_{1/2}$ was similar between plasma and milk. The time at which the maximum concentration occurred (T_{max}) in milk (8 h) was greater than that in plasma (1 h) and blood (4 h) (Table 1 and Figure 2).

Dasatinib was the major drug-related component in the milk samples at 1, 4, 8, 12 and 24 h post-dose (Figure 3). A radio-profile from a 4-h rat plasma sample analyzed in a previous experiment (Christopher et al., 2008a), is shown here to illustrate the differences between the plasma and milk profiles. The time-concentration profile of dasatinib in milk paralleled that of total radioactivity, with the T_{max} for each occurring at 8 h (Figure 2). M13, a sulfate conjugate of dasatinib, and M20/M24, two monohydroxylated metabolites, appeared in milk at a relatively higher concentration than other metabolites (Figure 3). The structures of the metabolites detected in milk are presented in Figure 1.

Maternal and fetal tissue distribution by tissue excision. [^{14}C]-Dasatinib-derived radioactivity was extensively distributed in maternal tissues, with maximum concentrations occurring at 8 hour post-dose (Figure 4). In the assayed maternal tissues, the radioactivity was highest in lungs, kidneys, liver and placenta, followed with heart, uterus, ovaries and blood, and lowest in cerebrum and amniotic fluid. The kinetic parameters are summarized in Table 2. The C_{max} value of [^{14}C]-dasatinib-equivalents in fetal blood was approximately 39% of that in maternal blood. The AUC values were comparable between fetal and maternal blood. The terminal $t_{1/2}$ in fetal blood was longer than that in maternal blood (Table 2, Figure 4). The concentrations of [^{14}C]-dasatinib-

equivalents in fetal kidney and liver were much lower than those in the respective maternal organs. The brain/blood ratios of C_{max} and $AUC_{0\text{-}inf}$ for fetus were approximately 1.58 and 1.48, which were much greater than 0.12 and 0.13 for maternal rats, respectively. Among all the tissues obtained from the fetuses, the exposures and kinetics of [^{14}C]-dasatinib-equivalents were comparable.

Maternal and fetal tissue distribution by QWBA. The tissue distribution results obtained by quantitative whole-body autoradiography were generally consistent with that by tissue excision. As shown in Figure 5, the distribution of [^{14}C]-dasatinib-derived radioactivity was extensive in maternal tissues. Highest radioactivity was detected in maternal adrenal gland, mammary tissue, liver, spleen, trachea, salivary gland and renal cortex. Only maternal adrenal gland and maternal mammary tissues were still quantifiable at 72 hours post-dose. Radioactivity in the following tissues was below the quantitation limit (<30.7 ng [^{14}C]dasatinib equivalents/g): amniotic fluid, bone, cerebellum, cerebrum, eyes, lens of eye, reproductive fat, medulla, olfactory lobe, and spinal cord. In addition, the highest radioactivity was observed with gastrointestinal contents and bile, which is consistent with the oral route of drug administration and known biliary excretion (Christopher et al., 2008a).

As shown in Figure 5, low levels of radioactivity were detected in fetuses. The fetal concentration of [^{14}C]-dasatinib-equivalents was below the quantitation limit (30.7 ng [^{14}C]dasatinib equivalents/g) at 1 hour post-dose, and reached C_{max} at 12 hours post-dose. At 48 hours post-dose, the overall radioactivity in fetuses was below the quantitation

limit. The radioactivity in amniotic fluid was below the quantitation limit in all time points. The radioactivity in placenta was greater than that in the fetal and maternal blood.

Discussion

Dasatinib was extensively secreted into milk of lactating rats following oral administration. The milk AUC value of the [^{14}C]dasatinib-equivalents was approximately 25-fold greater than the plasma AUC value (Table 1, Figure 2). Dasatinib is highly bound to proteins in rat serum with an unbound fraction of 3% (Kamath et al., 2008). It is a basic compound with a pKa at ~ 6.8, and is also lipophilic, with a log D of approximately 3.1 at pH 7-9 (Derbin G, personal communication). Estimation of the milk:plasma concentration ratio using a phase distribution model described by Atkison and Begg (Atkinson and Begg, 1990), predicted a slight concentration of dasatinib in milk (approximately 2-fold) by passive diffusion. Although the calculation does predict a modest concentration in milk, the observed milk:plasma ratio was much higher, and strongly suggests that active transporter(s) are involved in the lacteal secretion of dasatinib. Recently, the breast cancer resistance protein (BCRP, ABCG2), a member of the ATP-binding cassette family of transporters, was shown to be responsible for milk secretion of several drugs such as topotecan, cimetidine, acyclovir and nitrofurantoin as well as dietary carcinogen and toxin, 2-amino-1-methyl-6-phenylimidazo[4,5-b]pyridine (Jonker et al., 2005; Merino et al., 2005). BCRP is highly expressed and highly induced in the apical epithelial cells of the mammary gland during late pregnancy, and in particular during lactation as demonstrated in the mouse, cow and human (Jonker et al., 2005). During involution following cessation of lactation, the expression of BCRP in

mouse declined rapidly. In comparison, other efflux transporters such as p-glycoprotein, Mrp1 and Mrp 2 were found to be absent from breast tissue in lactating mouse, suggesting these efflux transporters may not be as important as BCRP in terms of lacteal secretion. BCRP is also responsible for the hepatobiliary secretion of a number of drugs and their metabolites (Hirano et al., 2005; Merino et al., 2005; Zamek-Gliszczynski et al., 2006; Ando et al., 2007). Although it is not currently known whether or not dasatinib is a substrate for BCRP, dasatinib and its metabolites were extensively secreted in bile of rats and monkeys (Christopher et al., 2008a), indicating that they may be substrates for this efflux transporter.

The parent compound was the predominant component of the drug-related radioactivity secreted into milk (Figure 3). In addition, relative to the plasma profile, the milk had a higher proportion of parent compound and lower percentages of metabolites. These data are also consistent with involvement of a transporter in the secretion of dasatinib into milk.

The distribution of dasatinib in maternal tissues was extensive, consistent with a high volume of distribution, reported previously (Kamath et al., 2008). The highest levels of radioactivity in maternal organs and tissues were associated with adrenal gland, lung, kidney, liver, placenta and mammary tissue. These maternal tissues had much higher levels of radioactivity than the maternal blood. The radioactivity in amniotic fluid was very low (Table 2, Figure 5). While concentrations of [^{14}C]dasatinib-equivalents in fetal kidney and liver were less than 13% of those in the respective maternal tissues, the exposures in the fetal organs were similar to fetal blood. These data suggest that

transporters may be involved in the uptake of dasatinib in maternal tissues; however, since these systems are not fully developed in the fetus, distribution to fetal tissues is predominantly mediated by diffusion.

The peak level of radioactivity in fetal blood was approximately 39% of that in maternal blood, but the overall AUC exposures were similar between fetus and mother (Table 2, Figure 4). This may be due to a relatively lower clearance in fetus, since the terminal $t_{1/2}$ in fetal blood was longer than that in maternal blood, or a slow time to achieve equilibrium across the placental barrier. It has been well-established that the placenta offers a protective barrier for the developing fetus by reducing the entry of exogenous compounds from mother to fetus (Syme et al., 2004). Several mechanisms play a role in placenta-blood barrier, including efflux transporters and drug metabolizing enzymes. Dasatinib has been shown to undergo extensive metabolism (Christopher et al., 2008a; Christopher et al., 2008b) and recently was shown to be a substrate of the p-glycoprotein (ABCB1, MDR1) efflux transporter (Giannoudis et al., 2008); both of these mechanisms may play a role in limiting fetal exposure.

It is noteworthy that the brain/blood ratio of [^{14}C]dasatinib-equivalents in the fetus is much higher than that in maternal rats (AUC: 1.48 vs. 0.13). For maternal rats, potential interactions of dasatinib with p-glycoprotein or other efflux transporters in the blood-brain barrier may be the mechanism for the low brain/blood ratio. However, some efflux transporters, including p-glycoprotein and BCRP are not expressed in the fetal blood-brain barrier at a comparable level to the adult (van Kalken et al., 1992). In the absence of efflux transporters in fetal blood-brain barrier, dasatinib presumably penetrates into brain

without efflux function. The higher than unity brain/plasma ratio in fetuses may be due to a higher affinity of dasatinib to brain tissue, as a result of its lipophilicity.

In summary, in pregnant or nursing rats, dasatinib was extensively distributed in maternal tissues and secreted into milk, but had limited brain penetration. Transporters such as BCRP and p-glycoprotein may play a role in the lacteal secretion, tissue distribution, and brain exclusion of dasatinib in the adult rat. However, drug-related radioactivity was more evenly distributed in fetal tissues, suggesting that these systems are not fully developed in the fetus. Although a complete fetal/neonatal risk-assesment would require comprehensive human studies, the data from the current study in rats would predict a significant exposure to the fetuses of pregnant women and infants of breast-feeding mothers undergoing dasatinib treatment.

Acknowledgments: We would like acknowledge Dr. George M. Derbin at Bristol-Myers Squibb Co. for providing procedures for formulation of dasatinib, Dr. Mingxin Qian for study design, and Dr. Milan Berge at Covance Co. for conducting the animal studies. We would also like to thank Drs. George Derbin and Michael J. Hageman (Bristol-Myers Squibb Co.) for helpful discussions about the physiochemical properties of dasatinib.

DMD Fast Forward. Published on September 11, 2008 as DOI: 10.1124/dmd.108.022764
This article has not been copyedited and formatted. The final version may differ from this version.

References

Allentoff A, Lago M, Ogan M, Chen BC, Zhao R, Iyer RA, Christopher LJ, Rinehart JK, Balasubramanian B and Bonacorsi J, S. J. (2008) Synthesis of ^{14}C-labeled and ^{13}C-, ^{15}N-labeled dasatinib and its piperazine *N*-dealkyl metabolite. *J. Label Compd. Radiopharm* **51:**41-47.

Ando T, Kusuhara H, Merino G, Alvarez AI, Schinkel AH and Sugiyama Y (2007) Involvement of breast cancer resistance protein (ABCG2) in the biliary excretion mechanism of fluoroquinolones. *Drug Metab Dispos* **35:**1873-1879.

Atkinson HC and Begg EJ (1990) Prediction of drug distribution into human milk from physicochemical characteristics. *Clin Pharmacokinet* **18:**151-167.

Atkinson HC, Begg EJ and Darlow BA (1988) Drugs in human milk. Clinical pharmacokinetic considerations. *Clin Pharmacokinet* **14:**217-240.

Christopher LJ, Cui D, Li W, Barros A, Jr., Arora VK, Zhang H, Wang L, Zhang D, Manning JA, He K, Fletcher AM, Ogan M, Lago M, Bonacorsi SJ, Humphreys WG and Iyer RA (2008a) Biotransformation of [^{14}C]dasatinib: in vitro studies in rat, monkey, and human and disposition after administration to rats and monkeys. *Drug Metab Dispos* **36:**1341-1356.

Christopher LJ, Cui D, Wu C, Luo R, Manning JA, Bonacorsi SJ, Lago M, Allentoff A, Lee FY, McCann B, Galbraith S, Reitberg DP, He K, Barros A, Jr., Blackwood-Chirchir A, Humphreys WG and Iyer RA (2008b) Metabolism and disposition of dasatinib after oral administration to humans. *Drug Metab Dispos* **36:**1357-1364.

Daley GQ, Van Etten RA and Baltimore D (1990) Induction of chronic myelogenous leukemia in mice by the P210bcr/abl gene of the Philadelphia chromosome. *Science* **247:**824-830.

Dorman DC, Allen SL, Byczkowski JZ, Claudio L, Fisher JE, Jr., Fisher JW, Harry GJ, Li AA, Makris SL, Padilla S, Sultatos LG and Mileson BE (2001) Methods to identify and characterize developmental neurotoxicity for human health risk assessment. III: pharmacokinetic and pharmacodynamic considerations. *Environ Health Perspect* **109 Suppl 1:**101-111.

Giannoudis A, Davies A, Lucas CM, Harris RJ, Pirmohamed M and Clark RE (2008) Effective dasatinib uptake may occur without human organic Cation Transporter 1 (hOCT1): implications for the treatment of imatinib resistant chronic myeloid leukaemia. *Blood*. epub.

Guilhot F, Apperley J, Kim DW, Bullorsky EO, Baccarani M, Roboz GJ, Amadori S, de Souza CA, Lipton JH, Hochhaus A, Heim D, Larson RA, Branford S, Muller MC, Agarwal P, Gollerkeri A and Talpaz M (2007) Dasatinib induces significant hematologic and cytogenetic responses in patients with imatinib-resistant or -intolerant chronic myeloid leukemia in accelerated phase. *Blood* **109:**4143-4150.

Hirano M, Maeda K, Matsushima S, Nozaki Y, Kusuhara H and Sugiyama Y (2005) Involvement of BCRP (ABCG2) in the biliary excretion of pitavastatin. *Mol Pharmacol* **68:**800-807.

Hochhaus A, Kantarjian HM, Baccarani M, Lipton JH, Apperley JF, Druker BJ, Facon T, Goldberg SL, Cervantes F, Niederwieser D, Silver RT, Stone RM, Hughes TP, Muller MC, Ezzeddine R, Countouriotis AM and Shah NP (2007) Dasatinib

induces notable hematologic and cytogenetic responses in chronic-phase chronic myeloid leukemia after failure of imatinib therapy. *Blood* **109:**2303-2309.

Jonker JW, Merino G, Musters S, van Herwaarden AE, Bolscher E, Wagenaar E, Mesman E, Dale TC and Schinkel AH (2005) The breast cancer resistance protein BCRP (ABCG2) concentrates drugs and carcinogenic xenotoxins into milk. *Nat Med* **11:**127-129.

Kamath AV, Wang J, Lee FY and Marathe PH (2008) Preclinical pharmacokinetics and in vitro metabolism of dasatinib (BMS-354825): a potent oral multi-targeted kinase inhibitor against SRC and BCR-ABL. *Cancer Chemother Pharmacol* **61:**365-376.

Lombardo LJ, Lee FY, Chen P, Norris D, Barrish JC, Behnia K, Castaneda S, Cornelius LA, Das J, Doweyko AM, Fairchild C, Hunt JT, Inigo I, Johnston K, Kamath A, Kan D, Klei H, Marathe P, Pang S, Peterson R, Pitt S, Schieven GL, Schmidt RJ, Tokarski J, Wen ML, Wityak J and Borzilleri RM (2004) Discovery of N-(2-chloro-6-methyl- phenyl)-2-(6-(4-(2-hydroxyethyl)- piperazin-1-yl)-2-methylpyrimidin-4- ylamino)thiazole-5-carboxamide (BMS-354825), a dual Src/Abl kinase inhibitor with potent antitumor activity in preclinical assays. *J Med Chem* **47:**6658-6661.

Lugo TG, Pendergast AM, Muller AJ and Witte ON (1990) Tyrosine kinase activity and transformation potency of bcr-abl oncogene products. *Science* **247:**1079-1082.

Merino G, Jonker JW, Wagenaar E, van Herwaarden AE and Schinkel AH (2005) The breast cancer resistance protein (BCRP/ABCG2) affects pharmacokinetics,

hepatobiliary excretion, and milk secretion of the antibiotic nitrofurantoin. *Mol Pharmacol* **67:**1758-1764.

Quintas-Cardama A, Kantarjian H, Jones D, Nicaise C, O'Brien S, Giles F, Talpaz M and Cortes J (2007) Dasatinib (BMS-354825) is active in Philadelphia chromosome-positive chronic myelogenous leukemia after imatinib and nilotinib (AMN107) therapy failure. *Blood* **109:**497-499.

Schittenhelm MM, Shiraga S, Schroeder A, Corbin AS, Griffith D, Lee FY, Bokemeyer C, Deininger MW, Druker BJ and Heinrich MC (2006) Dasatinib (BMS-354825), a dual SRC/ABL kinase inhibitor, inhibits the kinase activity of wild-type, juxtamembrane, and activation loop mutant KIT isoforms associated with human malignancies. *Cancer Res* **66:**473-481.

Shah NP, Lee FY, Luo R, Jiang Y, Donker M and Akin C (2006) Dasatinib (BMS-354825) inhibits KITD816V, an imatinib-resistant activating mutation that triggers neoplastic growth in most patients with systemic mastocytosis. *Blood* **108:**286-291.

Solon EG and Kraus L (2002) Quantitative whole-body autoradiography in the pharmaceutical industry. Survey results on study design, methods, and regulatory compliance. *J Pharmacol Toxicol Methods* **46:**73-81.

Syme MR, Paxton JW and Keelan JA (2004) Drug transfer and metabolism by the human placenta. *Clin Pharmacokinet* **43:**487-514.

Talpaz M, Shah NP, Kantarjian H, Donato N, Nicoll J, Paquette R, Cortes J, O'Brien S, Nicaise C, Bleickardt E, Blackwood-Chirchir MA, Iyer V, Chen TT, Huang F,

Decillis AP and Sawyers CL (2006) Dasatinib in imatinib-resistant Philadelphia chromosome-positive leukemias. *N Engl J Med* **354:**2531-2541.

Tokarski JS, Newitt JA, Chang CY, Cheng JD, Wittekind M, Kiefer SE, Kish K, Lee FY, Borzillerri R, Lombardo LJ, Xie D, Zhang Y and Klei HE (2006) The structure of Dasatinib (BMS-354825) bound to activated ABL kinase domain elucidates its inhibitory activity against imatinib-resistant ABL mutants. *Cancer Res* **66:**5790-5797.

van Kalken C, Giaccone G, van der Valk P, Kuiper CM, Hadisaputro MM, Bosma SA, Scheper RJ, Meijer CJ and Pinedo HM (1992) Multidrug resistance gene (P-glycoprotein) expression in the human fetus. *Am J Pathol* **141:**1063-1072.

Zamek-Gliszczynski MJ, Nezasa K, Tian X, Kalvass JC, Patel NJ, Raub TJ and Brouwer KL (2006) The important role of Bcrp (Abcg2) in the biliary excretion of sulfate and glucuronide metabolites of acetaminophen, 4-methylumbelliferone, and harmol in mice. *Mol Pharmacol* **70:**2127-2133.

Footnotes:

Reprint request details:

Kan He

UniTris Biopharma Co.

399 Cailun Rd, Building 1, Zhangjiang Hi-Tech Park

Shanghai 201203, China

Email: kan.he@unitrispharma.com

Figure Legends:

Figure 1. Metabolite pathway showing the chemical structures of dasatinib (P) and its metabolites secreted into milk. An asterisk (*) indicates the position of the ^{14}C-radiolabel.

Figure 2. Time-concentration profiles of [^{14}C]-dasatinib-equivalents in blood, plasma and milk in lactating Sprague Dawley rats on 8 or 9 days postpartum following a single oral dose of [^{14}C]dasatinib (10 mg/kg, 300 μCi/kg).

Figure 3. Representative HPLC-radiochromatograms of extracted milk samples collected at 1, 4, 8, 12 and 24 h post-dose and a plasma sample obtained 4 h post-dose. The radioactive peaks were identified based on mass fragmentation patterns and HPLC retention times as compared to previously identified metabolites. A radioprofile from a 4-h rat plasma sample analyzed in a previous experiment (Christopher et al., 2008a), is shown in the bottom panel to illustrate the differences between the plasma and milk profiles. The structure of dasatinib and its metabolites secreted into milk are shown in Figure 1.

Figure 4. Time-tissue concentration profiles of [^{14}C]-dasatinib-equivalents in maternal and fetal tissues in pregnant Sprague Dawley rats on gestation day 18 following a single oral dose of [^{14}C]dasatinib (10 mg/kg, 300 μCi/kg). Tissues were excised and radioactivity was determined by liquid scintillation counting.

Figure 5. Representative whole-body autoradiograph of radioactivity in a pregnant Sprague Dawley rat on gestation day 18, at 12 h after a single oral dose of [^{14}C]dasatinib

(10 mg/kg, 300 μCi/kg). Selected body sections are presented to demonstrate the distribution to various organs and tissues.

DMD Fast Forward. Published on September 11, 2008 as DOI: 10.1124/dmd.108.022764
This article has not been copyedited and formatted. The final version may differ from this version.

Table 1. Pharmacokinetic parameters of [^{14}C]-dasatinib-equivalents in blood, milk, and plasma of lactating Sprague Dawley rats on day 8 or 9 postpartum following a single oral dose of [^{14}C]dasatinib (10 mg/kg, 300 μCi/kg).

	C_{max} (ng equivalents/g)	T_{max} (hours)	$t_{1/2}$ [a] (hours)	AUC_{0-t} (ng equivalents × hour/g)	AUC_{0-inf} (ng equivalents × hour/g)
Blood	92.5	4	6.8	1,080	1,190
Milk	2,070	8	5.5	25,500	25,500
Plasma	96.0	1	7.6	1,020	1,150

[a] $t_{1/2}$ values were calculated using 3 time points.

DMD Fast Forward. Published on September 11, 2008 as DOI: 10.1124/dmd.108.022764
This article has not been copyedited and formatted. The final version may differ from this version.

Table 2. Kinetic parameters of [^{14}C]-dasatinib-equivalents in maternal and fetal tissues in pregnant Sprague Dawley rats on gestation day 18 following a single oral dose of [^{14}C]dasatinib (10 mg/kg, 300 μCi/kg).

Matrix	C_{max} (ng equivalents/g)	T_{max} (hours)	$t_{1/2}$ [a] (hours)	AUC_{0-t} (ng equivalents × hour/g)	AUC_{0-inf} (ng equivalents × hour/g)
Amniotic fluid	22.6	12	27	858	1,030
Blood	102	8	10	1,520	1,570
Cerebrum	12.1	8	18	190	363
Heart	322	8	12	4,800	4,830
Kidneys	1,060	8	16	15,900	16,300
Liver	878	8	19	16,700	17,200
Lungs	1,350	8	12	17,300	17,400
Ovaries	250	8	13	4,060	4,140
Placenta	551	8	15	11,400	11,900
Plasma	88.7	8	14	1,430	1,460
Uterus	271	8	8.9	4,260	4,400
Fetal blood	39.5	12	14	1,220	1,270
Fetal brain	62.4	8	14	1,810	1,880
Fetal kidneys	109	8	12	1,410	2,150
Fetal liver	112	8	5.9	2,150	2,170
Fetus (residual)	85.6	8	11	2,330	2,370

[a] $t_{1/2}$ values were calculated using 3 data points.

DMD Fast Forward. Published on September 11, 2008 as DOI: 10.1124/dmd.108.022764
This article has not been copyedited and formatted. The final version may differ from this version.

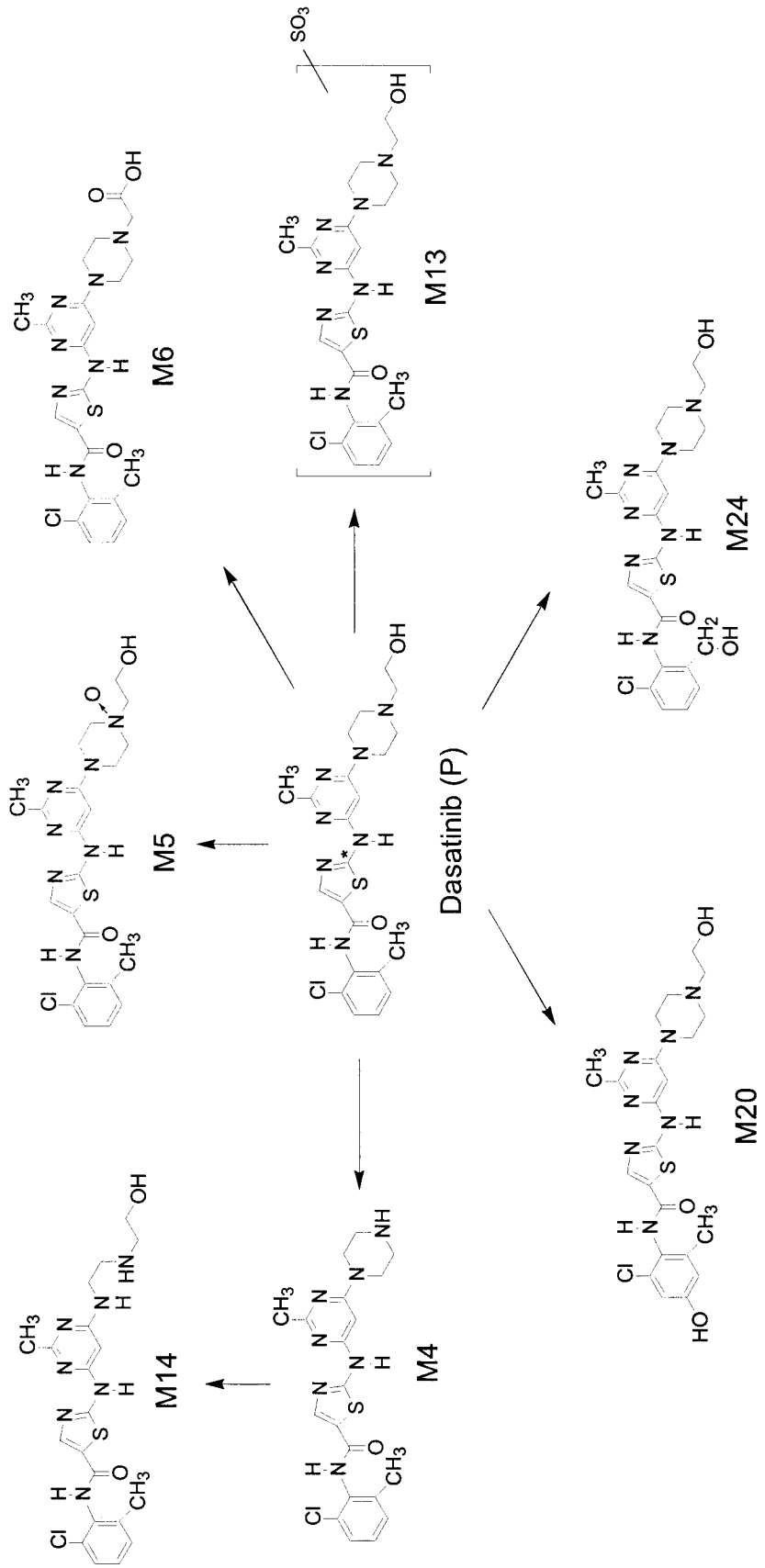

Figure 1

DMD Fast Forward. Published on September 11, 2008 as DOI: 10.1124/dmd.108.022764
This article has not been copyedited and formatted. The final version may differ from this version.

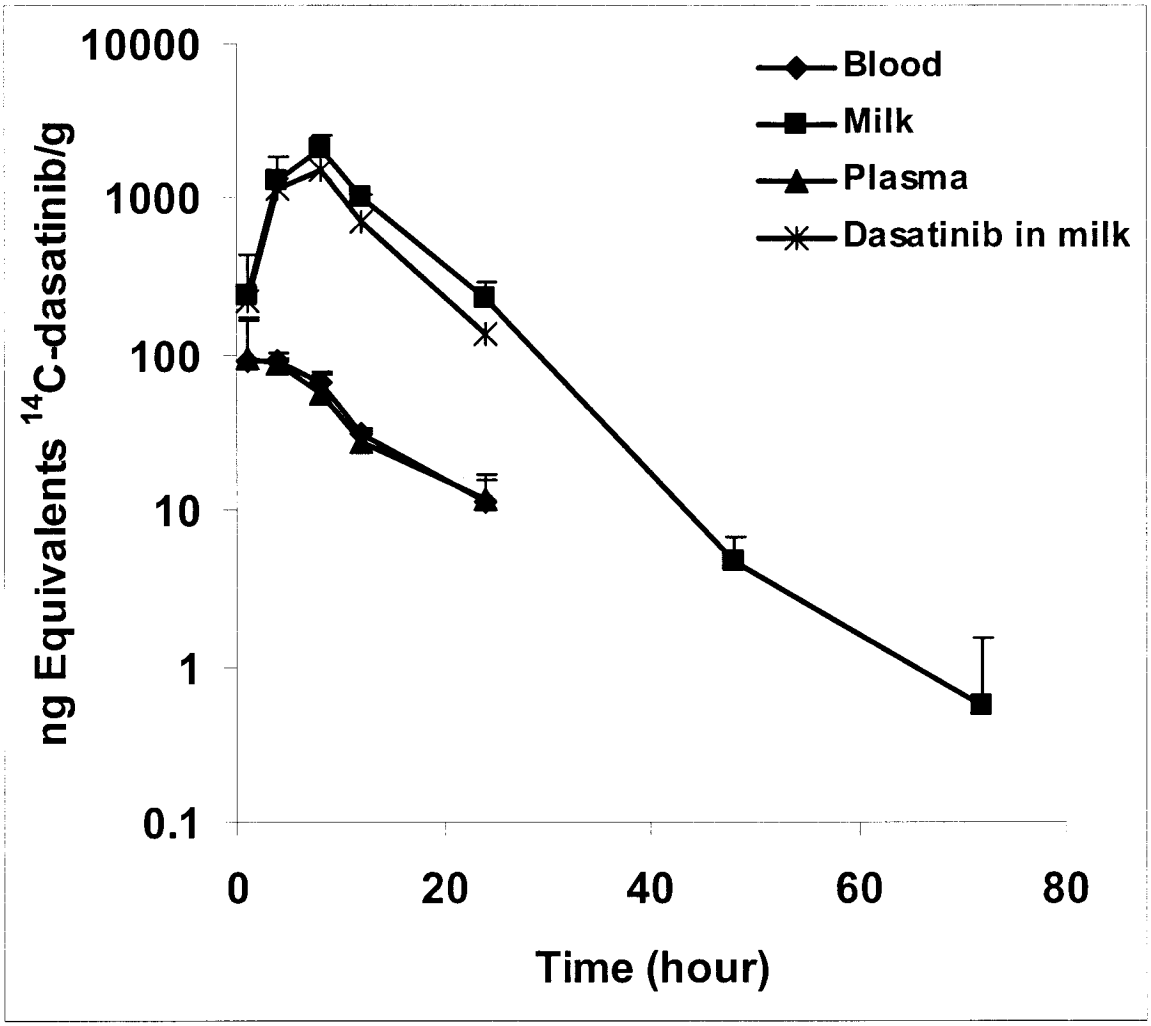

Figure 2

DMD Fast Forward. Published on September 11, 2008 as DOI: 10.1124/dmd.108.022764
This article has not been copyedited and formatted. The final version may differ from this version.

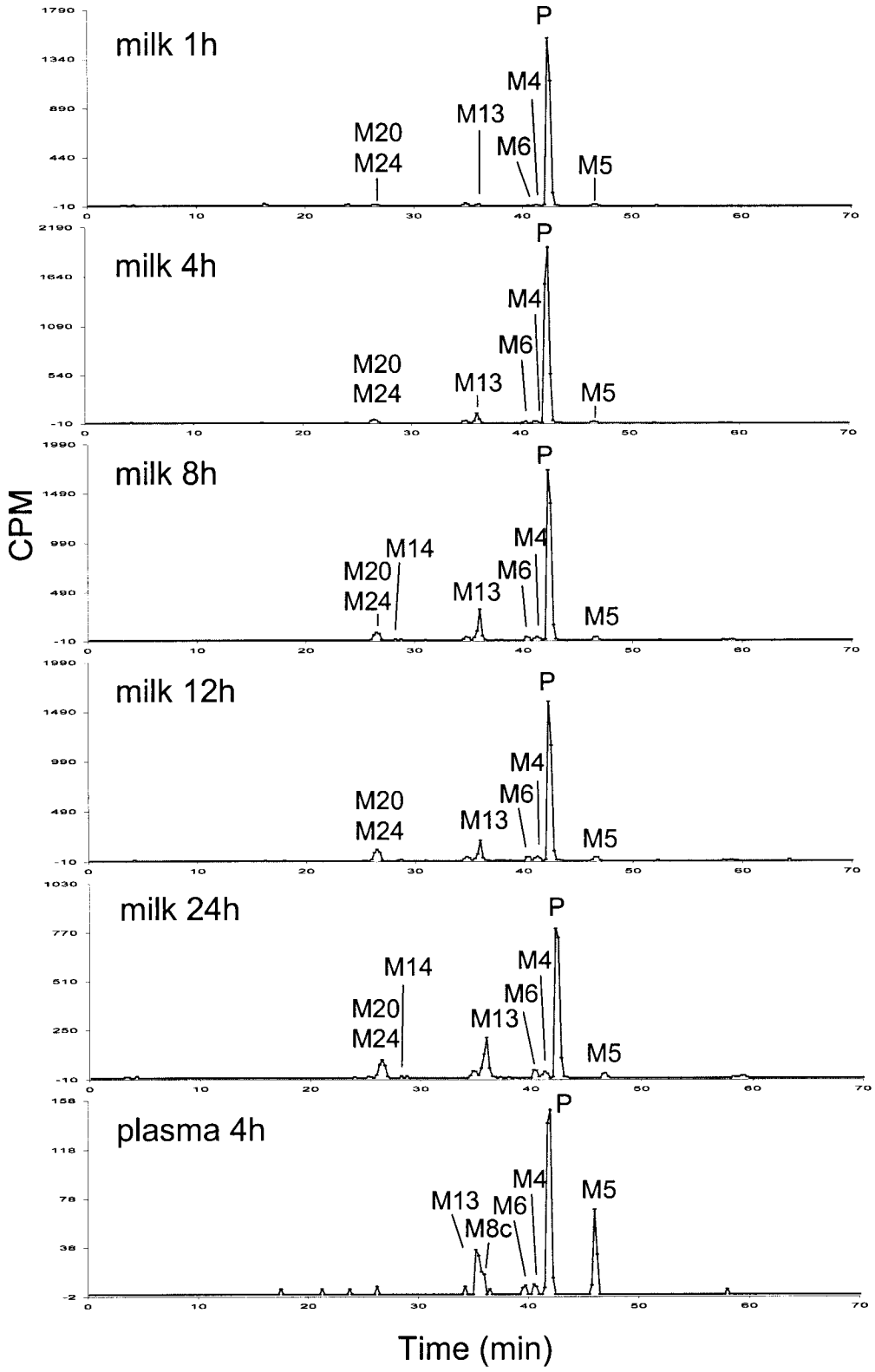

Figure 3

DMD Fast Forward. Published on September 11, 2008 as DOI: 10.1124/dmd.108.022764
This article has not been copyedited and formatted. The final version may differ from this version.

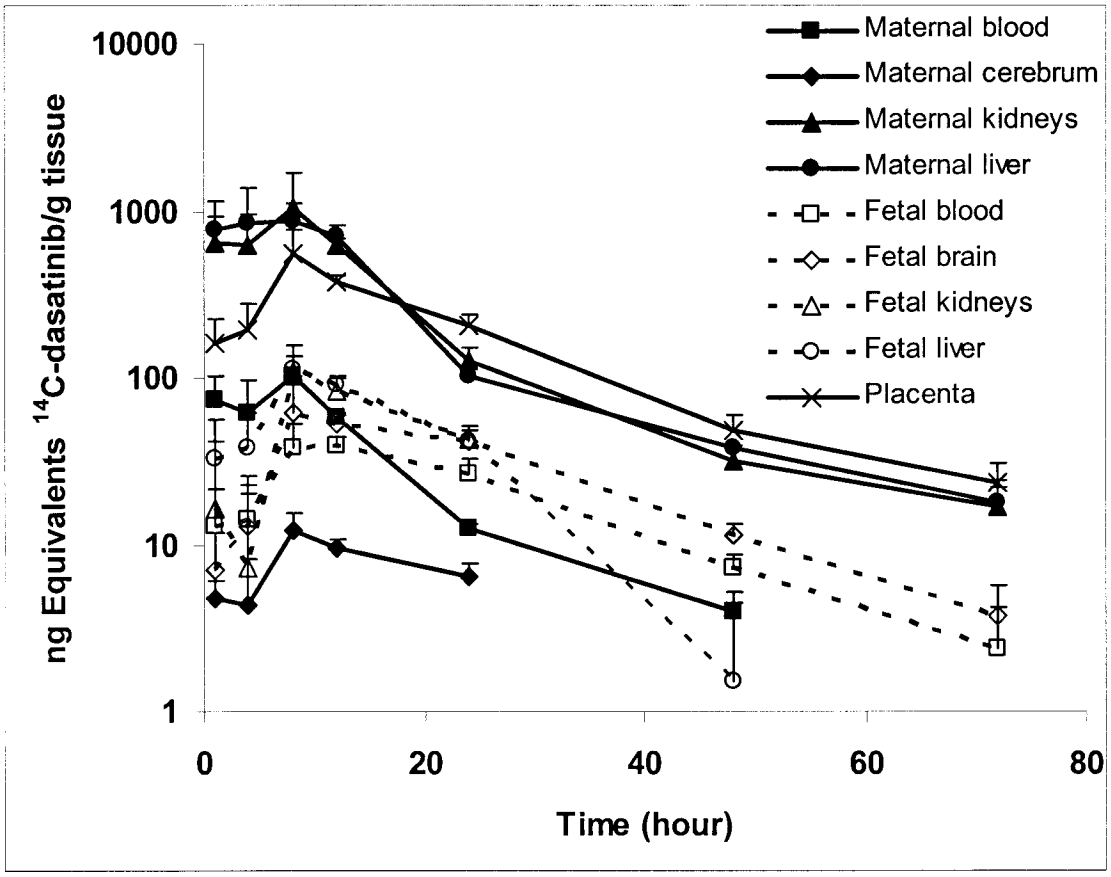

Figure 4

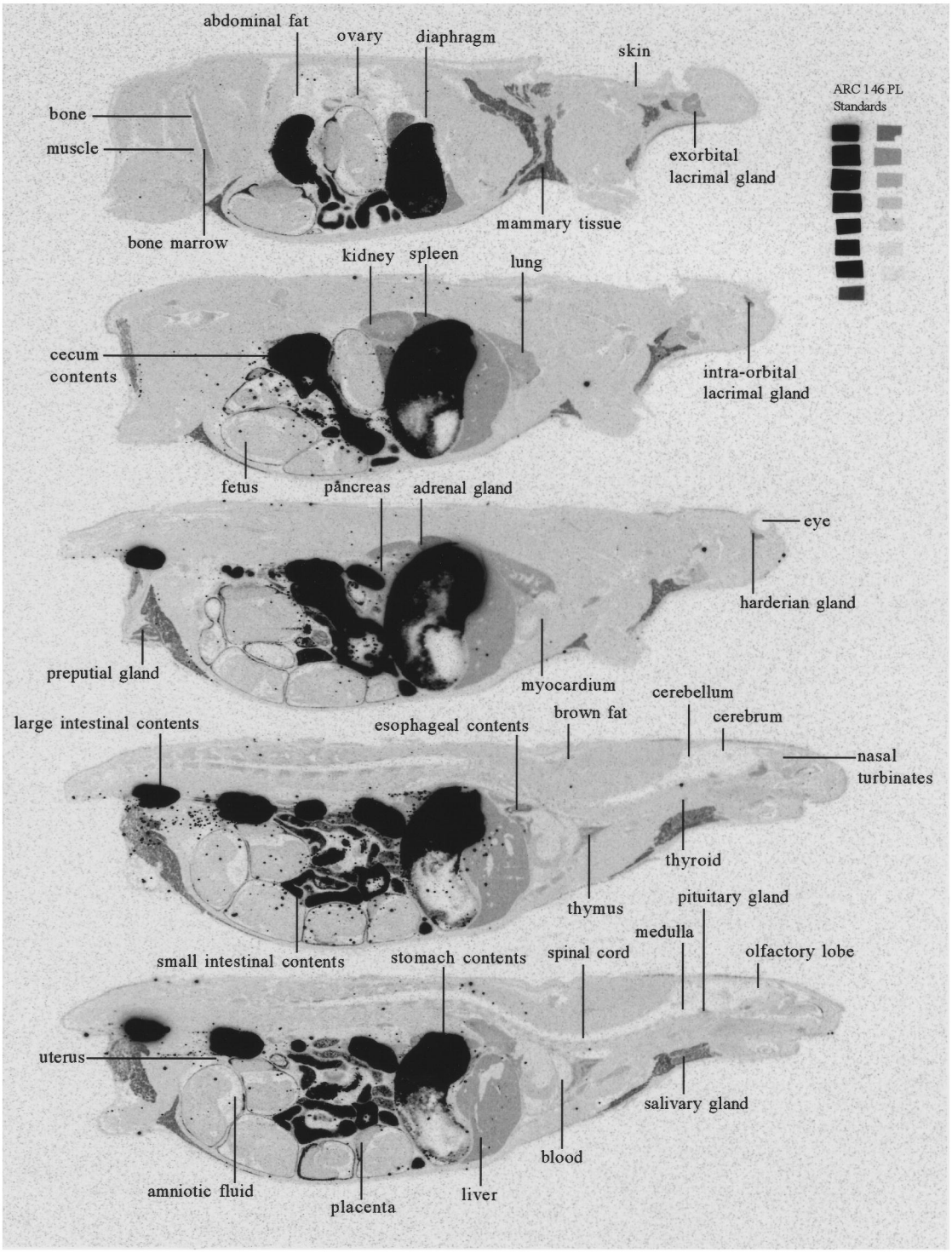

Figure 5